

Transition metal catalysts for molecular motors: towards molecular lithography

This article has been downloaded from IOPscience. Please scroll down to see the full text article.

2006 J. Phys.: Condens. Matter 18 S1909

(<http://iopscience.iop.org/0953-8984/18/33/S09>)

View [the table of contents for this issue](#), or go to the [journal homepage](#) for more

Download details:

IP Address: 129.252.86.83

The article was downloaded on 28/05/2010 at 12:59

Please note that [terms and conditions apply](#).

Transition metal catalysts for molecular motors: towards molecular lithography

Vincent Huc

Laboratoire de Chimie Inorganique, Université de Paris-Sud, bâtiment 420, 91405 Orsay cedex, France

E-mail: vincenthuc@icmo.u-psud.fr

Received 20 December 2005, in final form 7 March 2006

Published 4 August 2006

Online at stacks.iop.org/JPhysCM/18/S1909

Abstract

It is suggested that some transition metal based catalysts can be converted to molecular motors providing that their substrate is grafted onto a surface as a self-assembled monolayer.

This approach may open new possibilities, such as the control of molecular motion and chemical reactivity at a sub-nanometre scale under the influence of macroscopic controls such as electric fields, liquid crystal phases or light beams. Such a control may ultimately lead to molecular lithography.

First experimental results towards that goal are described in the last part of the paper.

(Some figures in this article are in colour only in the electronic version)

Historically, the concept of a ‘molecular machine’ was originally proposed by Richard Feynman 45 years ago [1]. During the last two decades, progresses in molecular biology made possible both the discovery of several families of moving proteins, and the elucidation of their motion mechanisms [2]. One of the most striking features is the similarity between the way these proteins are working at the molecular scale and our macroscopic machines. But the realization of artificial molecular (or supramolecular) systems undergoing a reversible and controlled mechanical deformation under the influence of a suitable energy input appeared more recently [3].

In order to keep the considerations and results developed in this paper accessible to different scientific backgrounds, simple recalls will be provided as often as necessary. In the first part of the paper, we will thus briefly describe the basics of molecular machines. In the last part, after a brief recall of their fundamental characteristics and properties, we will see how some well known chemical objects, ‘transition metal catalysts’, can be considered as a new huge family of molecular motors under certain conditions, opening unprecedented new possibilities.

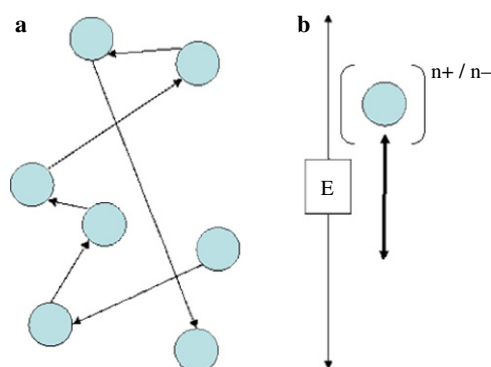


Figure 1. Brownian motion (a) and electrophoresis (b): diffusion-controlled processes.

1. What is a ‘molecular machine’?

A molecular machine may at first be considered as a system allowing a displacement of matter at the molecular scale, providing that a suitable energy supply is introduced into the system. However, this definition is incomplete, as processes such as Brownian motion or electrophoresis may be included in this definition. These two processes are indeed diffusion controlled ones, described by a potential energy curve (figure 1). In the former case, when diffusion occurs onto a surface, the displacements of the system may be described by a potential energy surface, combining two spatial coordinates and one energy coordinate.

Let us now consider the simplest kind of molecular machine: the molecular motor. Such a system produces a controlled displacement of matter at the molecular scale, under the influence of a suitable energy-supplying process (e.g. a chemical reaction). These systems are thus described by a potential energy surface combining three coordinates:

- the atomic displacements,
- the chemical axis (i.e. the reaction coordinates),
- the overall free energy of the system.

Moreover, as each unitary displacement of the motor is powered by at least one chemical reaction, a continuous motion of the motor implies successive chemical steps, resulting in a periodic potential energy surface (figure 2(a), from reference [4]). It should be noted that in most cases, the molecular systems considered here are fluxional. Each cycle of the molecular motor may include several rapidly interconverting intermediate states (figure 2(b)). An example of such a fluxional system is shown in figure 2. In this example, the system fluctuates between the three stable states A, B and C [4]. In order to obtain a directional motion, at least one of these interconversion steps is irreversible. The potential energy surface may be tilted along the position coordinate (figure 2(b)).

Let us now consider the intersection of the potential energy surface with the plane (free energy/reaction coordinate). The resulting periodic curve describes a chemical system undergoing a sequence of periodic, exothermic chemical transformations (without any mechanical displacement). It can thus be concluded that any system undergoing a cyclic sequence of globally exothermic chemical transformations may be ‘converted’ into a molecular motor, providing that:

- at least one chemical step of the cycle can be coupled with a mechanical displacement axis,

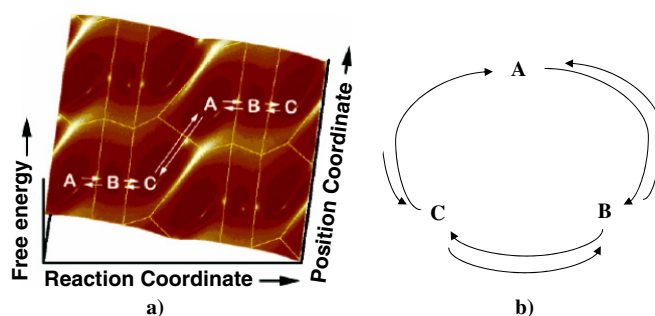


Figure 2. Potential energy surface (a) and corresponding chemical cycle (b) for a molecular motor. Reprinted with permission from [4]. Copyright 2001 American Chemical Society.

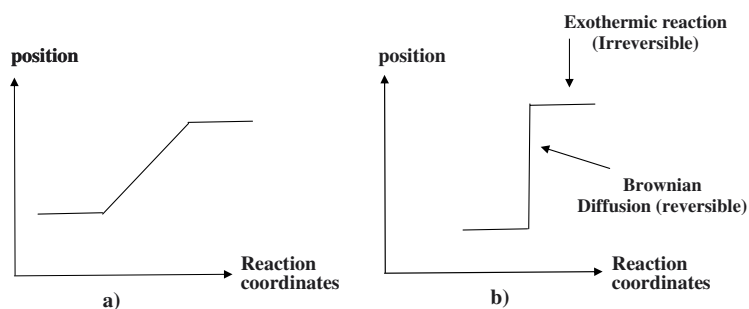


Figure 3. Converting chemical energy into a directional displacement: (a) power stroke; (b) molecular ratchet mechanisms.

- the mechanical displacement steps are occurring in a defined direction, resulting (on average) in a directed motion.

2. Molecular motors: how to make them work

There are two different ways to get the necessary coupling between the position axis and the chemical axis (figure 3). The first one is the so-called ‘power stroke’ mechanism. In this case, an exothermic chemical reaction directly induces the molecular displacement as it runs along the reaction coordinates axis (figure 3(a)). The second one is the so-called ‘molecular ratchet’ mechanism. In this case, the displacements along the reaction axis and the position axis are obtained independently (figure 3(b)). The displacement along the position axis results from a random, Brownian type diffusion.

3. Transition metal catalysts and molecular machines

Transition metal catalysts can be defined as compounds containing at least one transition metal atom that strongly accelerates a given chemical reaction. One possible acceleration mechanism occurs when the transition metal ion is able to activate at least one of the reagents by binding it into its own coordination sphere. Once the reaction is completed, the transition metal ion is recovered unchanged. An oversimplified description of such a process is shown in figure 4, in the simple case of a bimolecular $A + B$ reaction. Obviously, a direct analogy

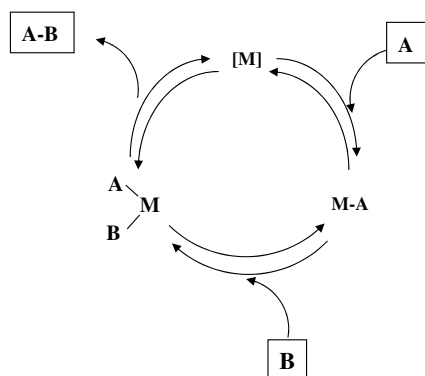


Figure 4. An example of a transition metal activated bimolecular reaction.

exists between the catalytic cycle shown in figure 4 and the one depicted in figure 2(b): these catalytic systems are undergoing a cyclic, ‘unidirectional’ motion along the chemical reaction axis (if the overall balance of the chemical cycle is exothermic). Such systems may thus be converted into molecular motors if they can be coupled with a mechanical displacement, while ensuring that these elementary displacement steps are directional. How may such a coupling be envisioned?

3.1. Combining a catalytic process and a molecular displacement

A simple solution is to bind one of the reagents (considered now as the ‘chemical fuel’) onto a topologically rigid substrate. In this case, solution-phase diffusion of the reagent to the catalyst is suppressed. Under these conditions, Brownian-assisted ‘jumps’ of the catalyst from one molecule to the next one over the substrate result in the expected coupling between the chemical reaction and the mechanical displacement. If the chemical reaction catalysed by the transition metal is irreversible (exothermic) and produces a potential barrier associated with back motion, the catalyst cannot move back, resulting in a unitary displacement. This simple description accounts for a ‘molecular ratchet’ type motion for the catalyst. However, a ‘power stroke’ type conversion is also possible, if the chemical reaction itself induces atomic displacements.

Combining a transition metal based catalytic process with a molecular displacement may be successful providing that four more conditions are fulfilled.

- (1) The first is that the catalyst should be kept in close proximity with the fuel molecules during the entire reaction; otherwise the catalytic motor will escape to the solution and will be lost for the process.
- (2) The second is that the distance between two adjacent fuel molecules should not be too high.
- (3) The third is that a matching is required between the catalyst’s motion on the rigid substrate and the rate of the catalytic process envisioned. For a ‘Brownian ratchet’ type mechanism, the Brownian step should not be too fast compared with the kinetic constant of the chemical process; otherwise some fuel molecules will be left unreacted behind the catalyst. The catalyst may then move backwards, and it will no longer be possible to ensure the motion’s directionality. In this case, the catalyst may also be ‘trapped’ between two already used fuel molecules (figure 5).
- (4) The ‘fuel molecules’ are organized on the substrate, in order to define favoured direction(s) of motion.

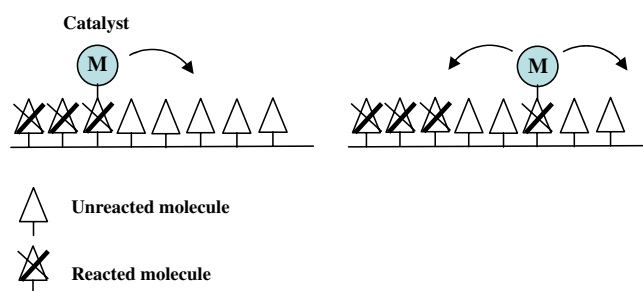


Figure 5. No directionality if the catalyst's motion is too fast compared with the kinetic constant of the chemical reaction.

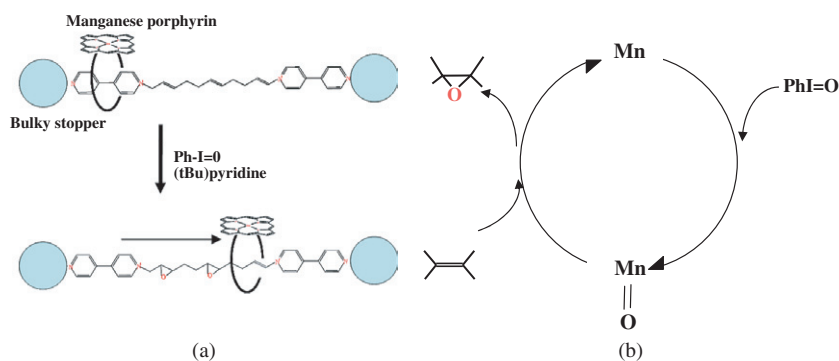


Figure 6. (a) Motion of a manganese porphyrin along a polymeric backbone powered by a catalytic epoxidation reaction; (b) corresponding catalytic cycle for the epoxidation reaction.

3.2. The rotaxane strategy

A first experimental approach is to bind one of the reagents involved in the catalytic cycle onto a polymer. Such an approach (reminiscent of some bio processes [5]) is exemplified by the work of Thordarsson, Rowan, Nolte *et al* [6]; see figure 6(a). Here, the catalytic process is an alkene epoxidation reaction, and the catalytic molecular motor is a manganese porphyrin. The overall catalytic cycle is depicted in figure 6(b). The catalyst is kept in close proximity with the 'chemical fuel' (the C=C double bonds) by threading it in a rotaxane-like fashion around the polymeric backbone. The two ends of the polymer are then capped with bulky groups, in order to prevent the catalyst from escaping to the solution. The catalytic molecular motor is first located on a specific chemical group at one end of the polymer (figure 6(a)). The catalytic process is then initiated by adding an activator for the bimolecular reaction (a pyridine type ligand) and the motor then starts moving. However, it is not clear at that point if the proposed system belongs to a processive or random type motion.

3.3. The surface strategy

Another possibility is to graft the molecules to be used by the catalyst as 'chemical fuel' onto a surface as a self-assembled monolayer (SAM), resulting in a periodic 2D molecular array. The catalytic motor may then move along this periodic array by jumping from one molecule to the next (figure 7). A very exciting possibility could be then to control the motion of the catalyst

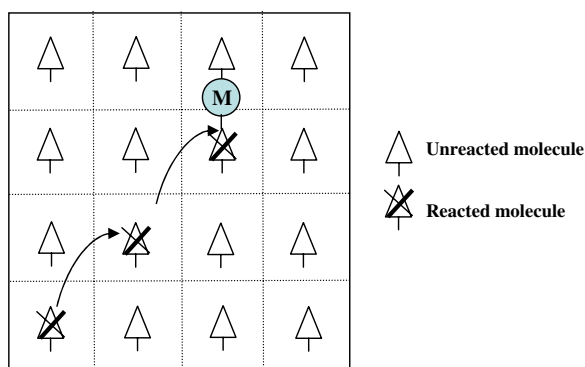


Figure 7. Chessboard-like motion of the catalyst on a self-assembled monolayer of reactive molecules.

as it moves on the plane, i.e. to control the catalyst's 'jumps' from one molecule to the next, in a 'chessboard-like' way (see section 5).

From the experimental point of view, satisfying the four conditions above (section 3.1) is more difficult in this case, one reason (among others) being that it may appear at first sight difficult to keep the catalyst on the SAM during the entire catalytic process. Fortunately, a specific subgroup of transition metal based catalysts, 'organometallic polymerization catalysts', provides elegant solutions to these problems. Let us now briefly recall the fundamentals of organometallic catalysts.

4. Organometallic catalysts for molecular motors

4.1. Organometallic catalysis: basic principles

In a very general sense, organometallic catalysts may be described as molecules containing a transition metal-to-carbon bond, prone to accelerate a given organic reaction. These catalytic systems are often very efficient, as one single molecule of organometallic catalyst may perform the transformation of hundreds of thousands of a given organic molecule in the most favourable cases, justifying their widespread use in laboratories and industry. One of the most striking features is that the complex set of chemical transformations leading to the overall considered reaction generally occurs in the coordination sphere of a *single* ion of a suitable metal. A simple way to explain this is the following 'hands and tools' rule (figure 8).

First, a catalytically active metal has some available orbitals, able to interact with the molecule to be transformed (substrate). These orbitals may thus be considered as catalyst's 'hands' to catch and keep the substrate in its coordination sphere. Second, some available electrons are also needed, in order for the catalyst to perform bond breaking and bond forming chemical reactions. These electrons may thus be considered as the 'tools' the catalyst uses to perform the chemical transformations observed. These principles are illustrated in figure 8, with the example of the interaction between a metallic atom and a C=C double bond. It is then possible to illustrate the way these catalysts are working with two famous examples: the Ziegler–Natta process for the production of polyethylene (figure 9), and alkene metathesis for the formation of polymers (figure 10). Millions of tons per year of chemicals (polyethylene, rubbers, drugs . . .) are produced in such a way.

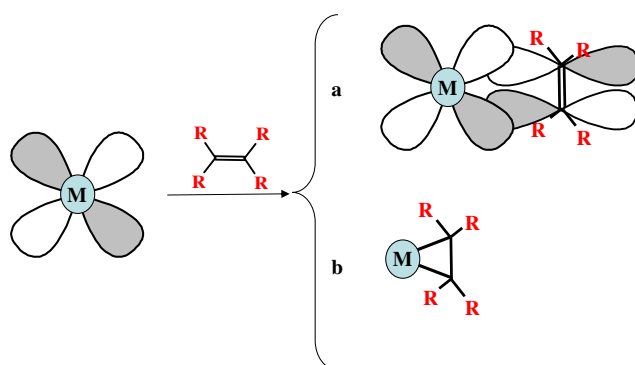


Figure 8. Basic principles for transition metal reactivity towards organic compounds: (a) interaction between the organic substrate and the metal via available orbitals of suitable symmetry; (b) bond forming reactions via available electrons of the metal.

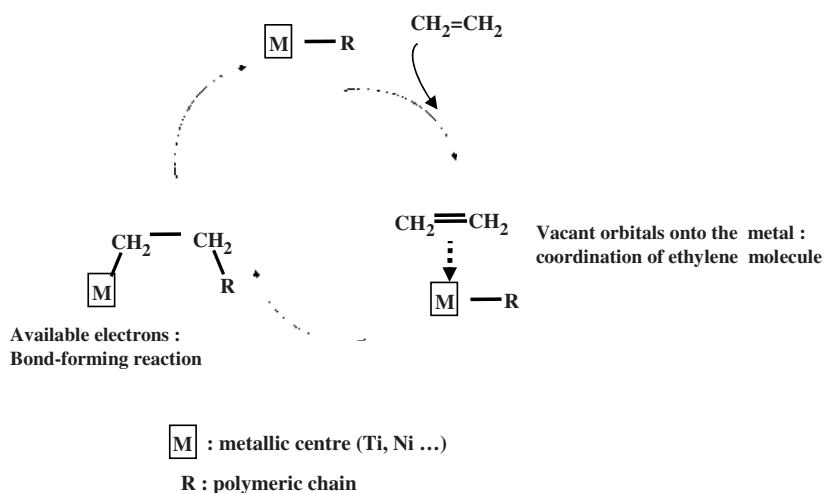


Figure 9. An example of an organic transformation catalysed by an organometallic catalyst: the Ziegler-Natta process for the polymerization of ethylene.

4.2. Polymerization catalysts: a family of molecular motor

The reactions shown in figures 9 and 10 are two examples (among many others) of *solution-phase*, organometallic catalyst based polymerization reactions. If now the molecules to be polymerized are *grafted* onto a surface as an organized SAM, the resulting 2D polymerization reaction will result in the motion of the catalyst from one molecule to the next on the surface, with simultaneous formation of a polymeric 'trace' behind it (figure 11) [7]. If the polymerization reaction is exothermic, the catalytic motor cannot move backwards, resulting in a unidirectional motion. The catalyst can now be considered as a molecular motor, powered by the chemical energy released by the reaction. In most cases, the way the chemical energy is converted into a mechanical displacement may combine both power stroke and Brownian ratchet type mechanisms. This approach appears quite general: any kind of organometallic polymerization catalyst may behave as a molecular motor under these conditions. This

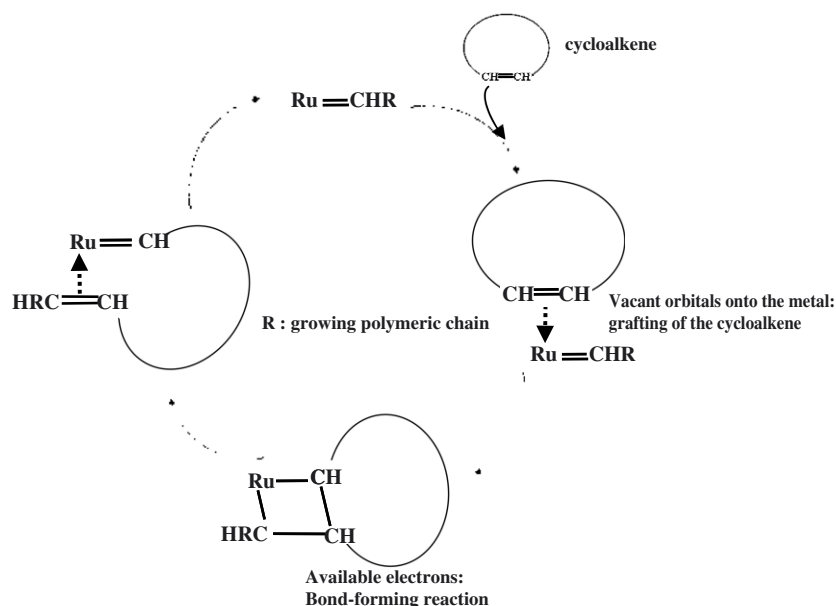


Figure 10. An example of an organic transformation catalysed by an organometallic catalyst: polymerization of cycloalkenes by the alkene metathesis reaction.

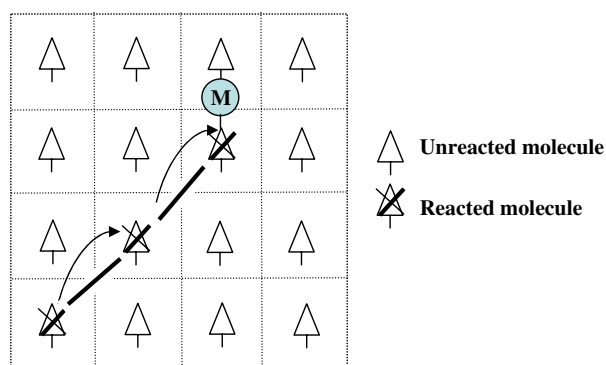


Figure 11. Motion of a polymerization catalyst along a self-assembled monolayer of reactive molecules. Formation of a polymeric trace.

‘organometallic catalysis’ based approach for the realization of molecular machines provides simple solutions to the four conditions mentioned above (section 3.1).

The first condition is automatically fulfilled in this case, due to the direct bonding that exists (in all organometallic polymerization reactions) between the molecular catalyst and the molecular fuel all over the process. The catalytic motor cannot escape to the solution and remains bonded to the surface. The second condition is also automatically satisfied, due to the compact assembly of the molecules to be polymerized as a self-assembled monolayer. The third condition is also automatically fulfilled in this case, once again because of the direct bonding that exists between the molecular catalyst and the molecular fuel during the entire process: *one* unitary ‘jump’ of the catalyst is automatically correlated with the consumption of *one* fuel molecule. Moreover, the organization of the ‘fuel molecules’ on the surface will very likely

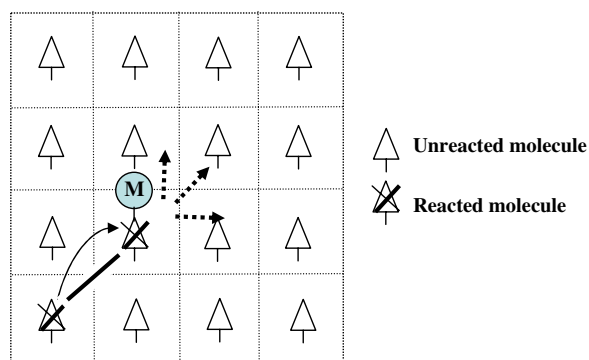


Figure 12. Different directions for a catalyst's 'jumps' from one molecule to the next.

induce favoured directions for the motion of the catalyst, due to differences in the accessibility (distances and orientations) of the reactive sites. The motion of the catalyst will thus be partly controlled by the organization of the molecules on the surface.

4.3. Probing the molecular motion

As already explained, the motion of the catalytic motor on the surface will result in the formation of a polymeric 'trace' on the surface. This phenomenon can be considered as a chemical bond displacement inside the SAM. If the starting monolayer can be imaged by STM, it should also be possible to evidence this molecular displacement by STM, by comparing the organization of the molecules on the SAM before and after reacting it with the catalyst.

5. Molecular lithography

A very interesting possibility is the control of the motion of the catalytic motor on the functionalized surface, i.e. to ultimately control each 'jump' of the catalyst from one molecule to the next (figure 12), in a chessboard-like way.

A first approach is to apply an external constraint to the motion of the catalyst. One possibility is to introduce an electric charge to the catalytic motor, and to control the motion by applying a parallel electric field to the surface [8]. Modifying the orientation of the electric field should result in a change of direction of the catalyst's displacement (figure 13).

Another possibility could be to run the whole process in the presence of a liquid crystalline phase above the SAM of 'fuel' molecules (figure 14). The highly anisotropic orientation of the molecules in the liquid crystal phase will induce a preferential direction for the motion of the catalyst. This effect may be observed if the catalyst is functionalized with large organic groups able to interact with the liquid crystal phase. As the orientation of the molecules in the liquid crystalline phase can be easily tuned by applying an electric field (or a polarized light) to the surface, the direction of motion of the catalyst should be controlled as well.

A second approach is to induce a change in the favoured direction of motion by reversibly modifying the organization of the 'fuel' molecules on the surface. Such a change may be induced thermally, for example by irradiating the surface with a laser.

Another possibility could be to use a SAM made of a 'fuel molecule' containing two distinct reactive sites. If the chemical reactivity of the most reactive of these sites can be modified (e.g. suppressed) by applying a suitable signal to the system (e.g. photochemical), the

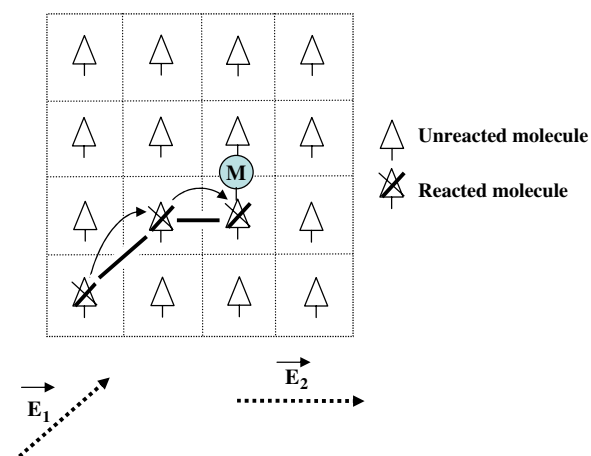


Figure 13. Controlled motion of the catalyst by applying an electric field parallel to the surface.

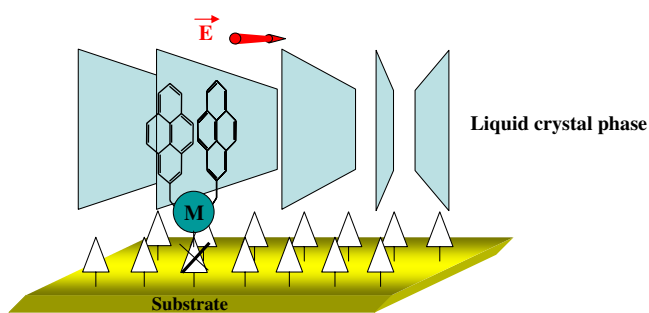


Figure 14. Controlling the motion of the catalyst with a liquid crystalline phase.

catalyst will ‘switch’ to the remaining active site, resulting in a modification of the favoured motion direction (figure 15). In this case, it should be necessary to synthesize a bifunctional fuel molecule containing two active sites for the polymerization reaction considered, the most reactive one being deactivated upon exposure to a suitable external stimulus.

Both approaches open two completely new possibilities. The first is ultimately the control of the displacements of a molecule (the catalyst) on a surface at the *sub-nanometre* scale (i.e. the distance between two adjacent fuel molecules on the SAM) under the influence of a *macroscopic* command (light beam, electric field ...). However, such a control should be possible only if the reaction kinetic associated with the catalyst’s ‘jumps’ from one molecule to the next on the surface is of the same order as the control process (photochemical, thermal ...). As the motion of the catalyst on the surface produces a characteristic ‘signature’ in the form a polymeric chain, a precise control of the motion of the catalyst is equivalent to controlling (at the same precision) a chemical reaction, in this case the structure and the organization of each polymeric chain on the surface.

This ‘molecular chessboard’ approach may thus open the possibility to build complex molecular objects on a surface in a very precise way (at the *sub-nanometre* scale) under the influence of a *macroscopic* control. The catalytic motor may thus be considered as a very precise molecular drawing tool under these conditions. This system opens the way to a true

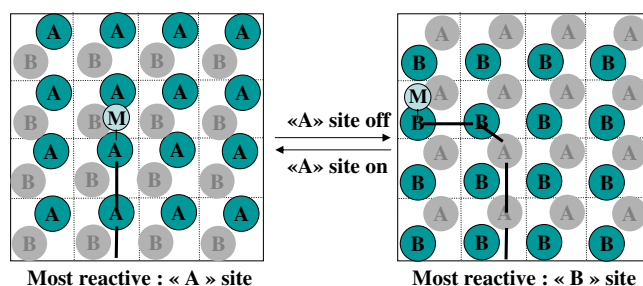


Figure 15. Controlled motion of the catalyst by using a 'chessboard' made of two different reactive sites, the most reactive one ('A') being reversibly deactivated.

'molecular lithography', in which molecular machines are used to draw, in a controlled way, complex nanometric structures on a surface, without the need for local probe instruments such as an STM or AFM.

6. First steps towards molecular lithography

6.1. Alkene metathesis: from synthetic organic chemistry to molecular machining

As already indicated, alkenes metathesis is now one of the most important organometallic catalysis based reactions. This reaction is widely used both in research and industry since the discovery of well defined Ru or Mo based efficient catalysts [9].

As shown in figure 10, this metathesis process may result in polymerizations, providing that a cycloalkene is used as the substrate. Considering the above discussion, it should thus be possible to turn the catalyst into a molecular motor, providing that the cycloalkene is grafted onto a surface.

Among all the known organometallic polymerization reactions, ruthenium based polymerization of norbornene derivatives (figure 16) is probably one of the most popular, due to its very high efficiency under ambient conditions, and the tolerance of the catalyst to air, moisture and most of the common organic functional groups. This system was thus chosen as a starting point.

The motion of one catalytic motor on an SAM of norbornene derivatives will thus result in the formation of a monomolecular polynorbornene chain (figure 16) [7]. Gold was chosen as the substrate, due to its well known surface chemistry and to the possibility of obtaining large atomically flat terraces. The synthesis of norbornene derivatives functionalized with sulfur-containing anchoring groups constitutes thus a first step. Moreover, as the packing of the norbornene derivatives on the surface may exert a great influence on the motion of the catalytic motor, we decided to start working with two different norbornene derivatives, in order to ensure a different organization for these two molecules on the surface. Comparative experiments with these two compounds should give more insights about the interplay between the organization of these 'fuel molecules' on the surface and the motion of the catalyst.

These two compounds are obtained according to straightforward synthetic schemes, depicted in figure 17. Very short alkyl chains are used to connect the sulfur anchoring atoms and the norbornene head groups in order to ease the STM imaging process. Compounds **A** and **B** are obtained in 80% and 20% yield respectively; detailed synthetic procedures are given in section 8.

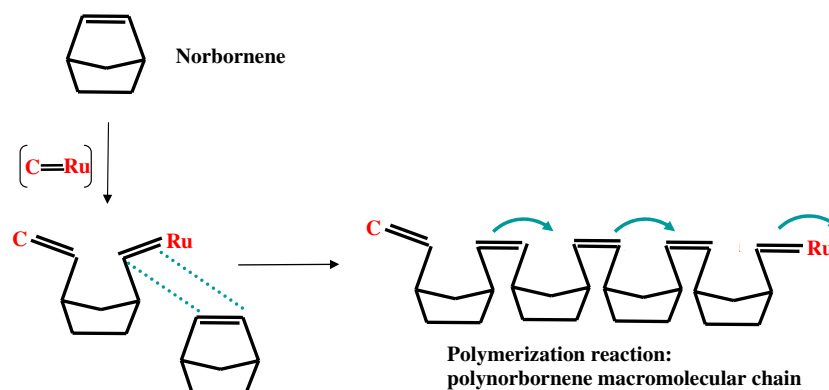


Figure 16. Norbornene polymerization induced motion of a ruthenium based molecular motor.

6.2. Self-assembly on gold surfaces

Figure 18 shows the IR spectra of bulk compound **A** (KBr pellet). The most important signals (1770 , 1700 and 1394 cm^{-1}) are associated with the $O=C-N-C=O$ imide vibrator. Figure 19 shows a schematic view of the most important modes (continuous line: atomic displacements) and the corresponding dipoles (dashed line) associated with the imide vibrator. The PM-IRRAS surface infrared spectra of a gold substrate after immersion in a solution of compound **A** is shown in figure 20. The expected characteristic signals are observed, confirming the successful grafting onto the surface. No evolution of the spectra is observed after sonicating the sample, revealing the formation of a very stable monolayer (figure 21). The comparison between the IR surface spectra shown in figure 21 and the bulk IR spectra depicted in figure 18 shows a marked increase in the relative intensity of the 1770 cm^{-1} imide $C=O$ symmetric stretching peak compared with the 1700 cm^{-1} imide antisymmetric $C=O$ stretching peak upon grafting onto the surface. The dipolar moment of the $C=O$ *antisymmetric* mode (figure 19(b)) has an important component *perpendicular* to the symmetry plane of the imide group, while the *symmetric* one is much smaller and has only one component *parallel* to the symmetry plane.

Considering that for a given vibrator close to a metallic surface, only the component of the dipole moment *perpendicular* to the surface contributes to the signal, it can thus be concluded that the imide group is oriented parallel to the gold surface (i.e. the oxygen–oxygen axis is parallel to the gold surface). Under these conditions, the difference between the signals associated with the symmetric and antisymmetric stretching modes is greatly reduced.

Similarly, a strong increase in the relative intensity of the imide $C-N$ symmetric stretching mode (1397 cm^{-1}) is observed (figure 20). As the corresponding dipole moment is oriented along the symmetry plane of the imide vibrator (figure 19(c)), this increase is also explained by a parallel orientation of the imide vibrator (referred to the oxygen–oxygen axis) to the gold surface.

It can thus be concluded that the norbornene groups are oriented in such a way that the symmetry plane of these groups is perpendicular to the surface (figure 22). The reduced projected surface area for the norbornene group in such an orientation results in both a higher surface coverage and a better molecular packing. The observation of these strong packing effects shows that the molecules are well organized in the monolayer (at least locally). The very anisotropic and rigid shape of the norbornene group probably accounts for these effects.

Obtaining a well organized SAM with molecules exhibiting a large difference between the area of the anchoring group (the sulfur atom) and the organic headgroup (the norbornenes) was

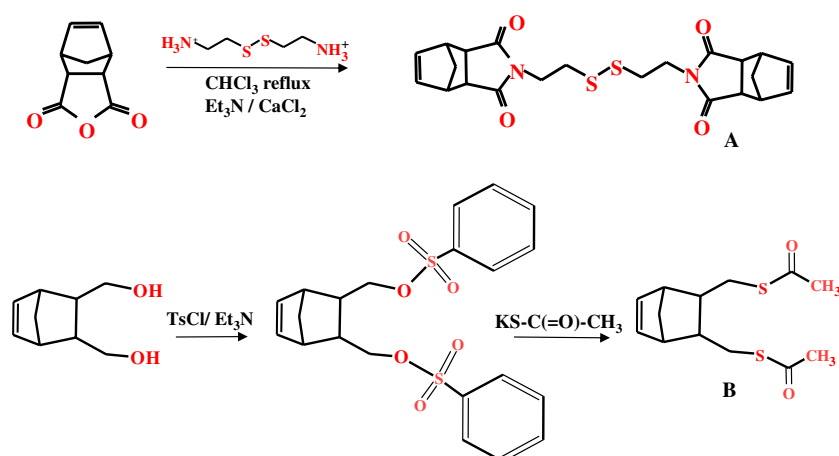


Figure 17. Synthesis of norbornene derivatives for self-assembly on gold substrates.

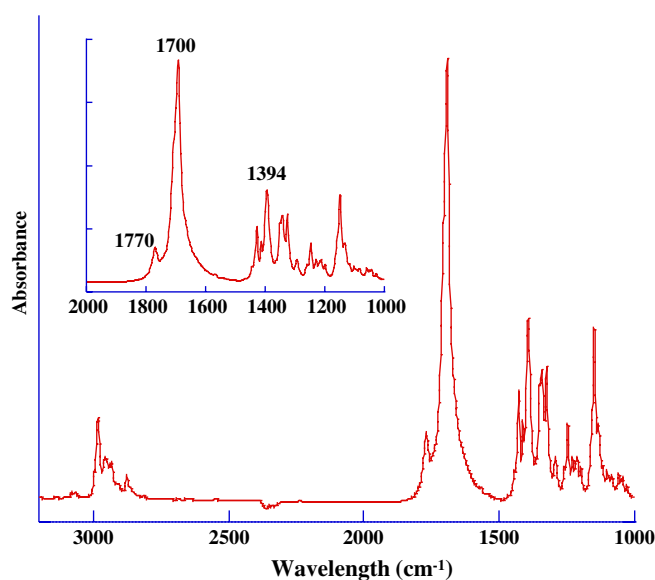


Figure 18. Infrared spectra of bulk A (KBr pellet).

not obvious at first sight. However, some examples of well organized SAMs with compounds exhibiting such difference (adamantanes) have already been described [10].

Figure 23 shows a liquid phase (octylbenzene) STM image of this monolayer. The presence of the characteristic etch pits on the surface shows that the self-assembly process has indeed occurred. The molecules are observed as bright spots (about 4–5 Å in diameter), uniformly covering the surface, and they are locally organized (figure 24).

Considering that the imaging process was done in the liquid phase, and the small size of the molecular ‘spots’ observed, the successful observation of the molecules shows that molecular motions are greatly reduced on the surface. This observation reveals a high intermolecular packing, in accordance with the spectroscopic data.

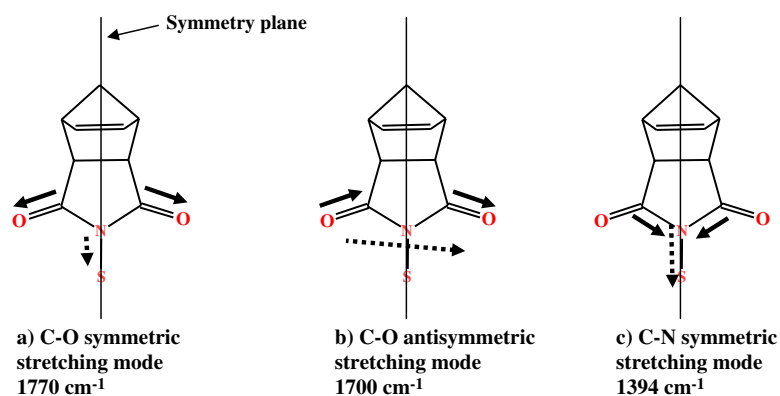


Figure 19. Most important vibrators associated with the imide group. Atomic displacements (continuous line). Corresponding dipole moments (dashed line).

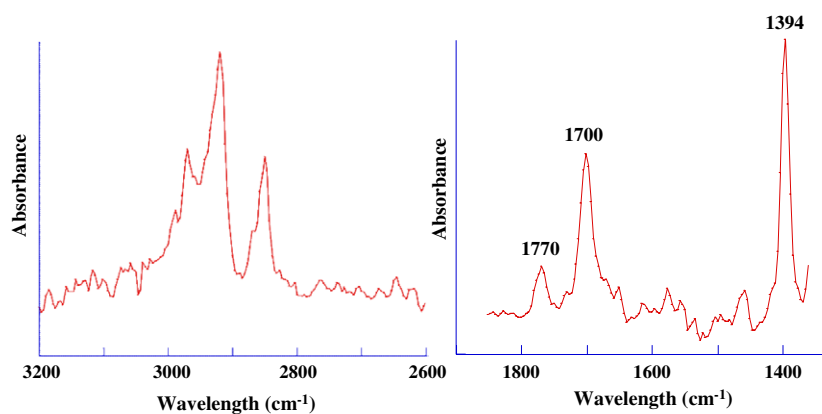


Figure 20. PM-IRRAS spectra of a self-assembled monolayer of compound A.

7. Conclusions and outlooks

It is interesting to see that an old and well known group of molecules may find surprising applications, if they are considered from a different point of view.

In the first part of this paper, we suggested that organometallic polymerization catalysts, a well known class of transition metal containing molecules, may be diverted from their initial use of catalysts for organic transformations, and converted to molecular motors providing that their organic substrate is grafted onto a surface. This approach opens new possibilities to control both molecular motion and chemical reactivity on a surface at the *sub-nanometre* scale under the influence of a *macroscopic* command. This new strategy was given the general designation of ‘molecular lithography’. Within this frame, some possible avenues of research are suggested.

In the second part of the paper, we described the first steps towards the experimental demonstration of this strategy. The synthesis of two new specifically designed norbornene derivatives, containing one (compound **A**) or two (compound **B**) anchoring groups for gold substrates was described. In the case of compound **A**, the formation of a robust SAM of organized molecules was demonstrated, and it was shown that STM imaging of these molecules is possible.

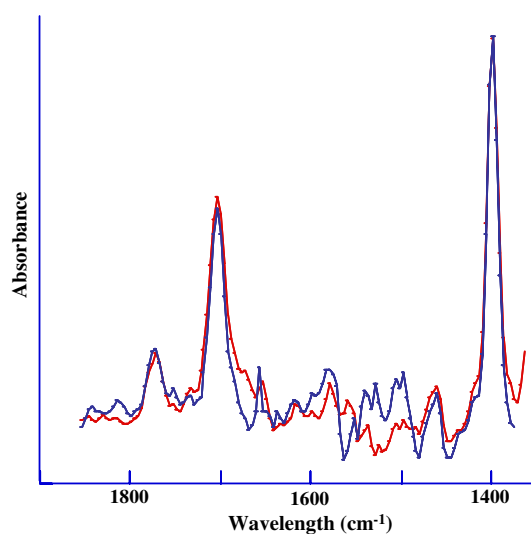


Figure 21. PM-IRRAS spectra of a self-assembled monolayer of compound A before and after sonication (CH₂Cl₂).

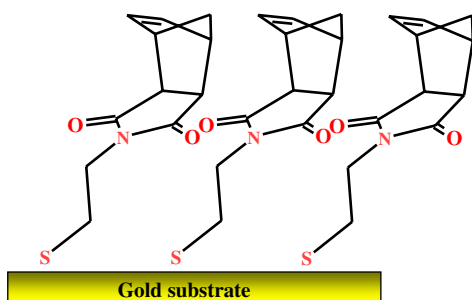


Figure 22. Proposed structure for the self-assembled monolayer of compound A.

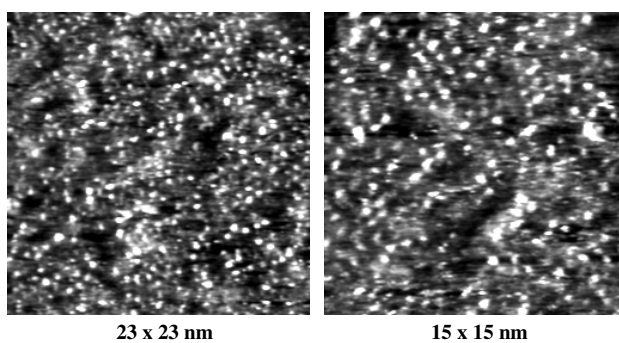


Figure 23. Liquid phase (octylbenzene) STM of a self-assembled monolayer of compound A.

Although the organization of the molecules on the surface is not perfect, the demonstration that a monolayer of a norbornene derivative can be successfully imaged by STM is of crucial importance for the next steps. The bis(thioester) **B** (figure 17) should lead to more organized molecular layers on gold substrates. The study of these monolayers is in progress.

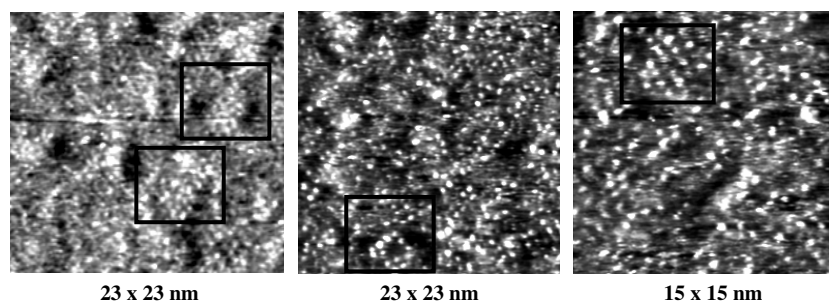


Figure 24. Liquid phase (octylbenzene) STM of a self-assembled monolayer of compound A: organization of the molecules on the surface.

As a closing remark, although many issues remain to be addressed to get an operational molecular lithography system, some encouraging steps towards that goal are demonstrated.

8. Experimental details

General.

All chemicals and solvents were purchased from Aldrich (reagent grade) and used as received. Bulk IR spectra were recorded with a Perkin-Elmer 1000 FT-IR spectrometer. PM-IRRAS reflection spectra were recorded with a Nicolet spectrometer. ES-MS were recorded with a MAT-95 spectrometer.

Synthesis of compounds A and B

Compound A. To a 250 ml round-bottomed flask, fitted with a CaCl_2 drying cartridge and a reflux condenser are added 100 ml of chloroform, 10 g of cystamine dihydrochloride, 20 g of carbic anhydride and 21 ml of triethylamine. The resulting solution is then refluxed for several hours, while the reaction is monitored by IR and RMN spectroscopy. Once the reaction is complete, the mixture is diluted with dichloromethane (100 ml), and filtered. The filtrate is then evaporated under reduced pressure and the product is purified by column chromatography (SiO_2 /dichloromethane). Compound A is obtained as a white solid. Yield: 80%. $^1\text{H RMN}$ (CDCl_3): 6.11 ppm, (s) 2H; 3.64 ppm, t 2H (3.37) and 3.27 ppm, (m) 4H; 2.74 ppm, (t) 2H; 1.7 ppm, (d) 1H; 1.55 ppm, (d) 1H. IR (KBr): 1770, w and 1700 (vs): imide C=O stretch. Mass spectrometry (ES-MS): $m/z = 445.2$ (MH⁺), 467.2 (MNa⁺), 483.2 (MK⁺).

Compound B.

(1) Synthesis of 5-norbornene-2-exo, 3-exo (ditosylate).

To a solution of 0.170 g of 5 norbornene-2-exo, 3-exo dimethanol in 3 ml THF and 1 ml triethylamine is added a solution of 0.5 g of tosyl chloride in 3 ml THF. After stirring overnight at ambient temperature, the resulting orange solution is filtered, and the product is purified by column chromatography (SiO_2 /dichloromethane/pentane 80/20 v/v). The product is obtained as colorless crystals.

$^1\text{H RMN}$ (CDCl_3): 7.72 ppm (d), 4H; 7.32 ppm (d), 4H; 6.03 (s), 2H; 4 ppm (m) 2H; 3.8 ppm, (m) 2H; 2.4 ppm (s) 3H; 1.8 ppm (m), 2H; 1.2 ppm (m), 2H

Mass spectrometry (ES-MS): $m/z = 485.1$ (MNa⁺)

(2) Synthesis of 5-norbornene-2-exo, 3-exo (dithioacetate) (compound **B**).

To a suspension of 160 mg of 5-norbornene-2-exo, 3-exo dithiosylate in 6 ml of DMSO is added 170 mg of potassium thioacetate and the resulting suspension is stirred for 3 days under an argon atmosphere at ambient temperature. The resulting pale yellow solution is diluted with water, and the resulting fine precipitate is collected by centrifugation. The precipitate is collected with dichloromethane and evaporated under reduced pressure. Compound **B** is obtained as pale yellow crystals in nearly quantitative yield. Overall yield: 20%.

¹H RMN (CDCl₃): 6.08 ppm (s), 2H; 3.2 ppm (m), 2H; 2.7 ppm (m), 4H, 2.33 ppm (s), 6H; 1.6 ppm (m), 3H, 1.33 ppm (d), 1H

IR (KBr): 1679.5 thioester C=O stretch

Mass spectrometry (ES-MS): $m/z = 293.2$ (MNa⁺)

Self-assembly of compound A on gold substrates. Gold substrates were cleaned by ozonolysis (30 min), washed with ethanol, dried under a nitrogen stream and submitted to a new 30 min ozonolysis period. The absence of any organic contaminant was checked by PM-IRRAS. The freshly cleaned gold substrates were then immersed for 24 h in a millimolar solution of compound A in a dichloromethane/ethanol (80/20 v/v) mixture. The substrates were then rinsed with dichloromethane, sonicated in dichloromethane and dried under a nitrogen stream.

STM imaging. The substrate was a 1000 nm thick layer of gold epitaxially grown on Mica so as to expose a (111) face. The tips were mechanically formed in a 250 μm Pt–Ir wire (Pt80/Ir20, Goodfellow). To avoid moisture contamination, the junction was immersed in a phenyl-octane droplet during STM operation. STM imaging was achieved through a home-made digital system. The images reported here were obtained in the current mode, with slow height regulation to a tunnel current of 35 pA, at a sample bias of –500 mV. The fast scan axis was kept perpendicular to the sample slope. Images acquired simultaneously in both scan directions were systematically recorded and compared.

Acknowledgments

Dr F Charra and Guillaume Schull are deeply acknowledged not only for recording the STM pictures, but also for their interest in this work and their dynamism. This will certainly be of the greatest importance in the future. Dr Henri Lezec (Institut des Sciences et d'Ingénierie Supramoléculaire, Strasbourg/France) is also warmly acknowledged for very stimulating discussions, that contributed to the ideas and concepts developed in this paper.

References

- [1] Feynman R P 1960 *Eng. Sci.* **23** 22
- [2] Holmes K C 1997 *Curr. Biol.* **7** R112
- Kitamura K, Tokunaga M, Iwane A H and Yanaguida T 1999 *Nature* **397** 129
- Bunk R, Klinth Montelius L, Nicholls I A, Omling P, Tagerud S and Mansson A 2003 *Biochem. Biophys. Res. Commun.* **301** 783
- Schliwa M (ed) 2003 *Molecular Motors* (Wenheim: Wiley–VCH)
- Boyer P D 1993 *Biochim. Biophys. Acta* **1140** 215
- Abrahams J P, Leslie A G W, Lutter R and Walker J E 1994 *Nature* **370** 621

- [3] Shinkai S 1987 *Pure Appl. Chem.* **59** 425
Shinkai S 1999 *Comprehensive Supramolecular Chemistry* ed G W Gokel (Oxford: Elsevier Science) pp 671–700
Koumura N, Zijlstra R W J, Van Delden R A, Harada N and Feringa B L 1999 *Nature* **401** 152
Matthijs K W, Richard A D, Auke M and Feringa B 2003 *J. Am. Chem. Soc.* **125** 15076
Kelly T R, De Silva H and Silva R A 1999 *Nature* **401** 150
Leigh D A, Wong J K Y, Dehez F and Zerbetto F 2003 *Nature* **424** 174
Bissel A, Cordova E, Kaifer A E and Stoddart J F 1994 *Nature* **369** 133
Balzani V, Credi A, Raymo F M and Stoddart J F 2000 *Angew. Chem. Int. Edn* **39** 3348
Badjic J D, Balzani V, Credi A, Silvi S and Stoddart J F 2004 *Science* **303** 1845
Jimenez-Molero C, Dietrich-Buchecker C and Sauvage J P 2000 *Angew. Chem. Int. Edn* **39** 3284
Jimenez-Molero C, Dietrich-Buchecker C and Sauvage J P 2003 *Chem. Commun.* 1613
Rapenne G 2005 *Org. Biomol. Chem.* **3** 1165
- [4] Bustamente C, Keller D and Oster G 2001 *Acc. Chem. Res.* **34** 412
- [5] Traskelis M A, Alley S C, Abdel-Santos E and Benkovic S J 2001 *Proc. Natl Acad. Sci. USA* **98** 8368
Kovall R and Matthews B W 1997 *Science* **277** 1824
- [6] Coumans R E, Elemans J W, Thordarsson P, Nolte R M and Rowan A E 2003 *Angew. Chem. Int. Edn* **42** 6
Thordarsson P, Bijsterveld E J A, Rowan A E and Nolte R M 2003 *Nature* **424** 915
- [7] Xue-Mei L, Huskens J and Reinhoudt D 2003 *Nanotechnology* **14** 1064
- [8] Asokan S B, Jawerth L, Carrol R L, Cheney R E, Washburn S and Superfine R 2003 *Nano Lett.* **3** 431
Horinek D and Michl J 2003 *J. Am. Chem. Soc.* **125** 11900
Huahua J and Tour J M 2003 *J. Org. Chem.* **68** 5091
- [9] For alkyne metathesis catalysts:
Schrock R, Murdzek G C, Bazan J R, Robbins J, DiMare M and O'Regan M 1990 *J. Am. Chem. Soc.* **112** 3875
Oskam J H, Fox H H, Yap K B, McConville D H, O'Dell R, Lichtenstein B J and Schrock R R 1993 *J. Organomet. Chem.* **459** 185
For alkene metathesis catalysts:
Nguyen S T, Johnson L K and Grubbs R H 1992 *J. Am. Chem. Soc.* **114** 3974
Schwab R H and Grubbs R H 1996 *J. Am. Chem. Soc.* **118** 100
For a general review:
Fürstner A 2000 *Angew. Chem. Int. Edn* **39** 3012
- [10] Dameron A A, Charles L F and Weiss P S 2005 *J. Am. Chem. Soc.* **127** 8697